

## Article

# Development of Reactive Power Allocation Method for Radial Structure Wind Farm Considering Multiple Connections

Deokki Yoo <sup>1</sup>, Sungwoo Kang <sup>1</sup>, Gilsoo Jang <sup>1,\*</sup> and Seungmin Jung <sup>2,\*</sup>

<sup>1</sup> Department of Electrical Engineering, Korea University, Anam-dong, Seongbuk-gu, Seoul 02841, Korea; deok403@korea.ac.kr (D.Y.); kswvoice@korea.ac.kr (S.K.)

<sup>2</sup> Department of Electrical Engineering, Hanbat National University, Daejeon 34158, Korea

\* Correspondence: gjang@korea.ac.kr (G.J.); seungminj@hanbat.ac.kr (S.J.)

**Abstract:** In recent years, the number of wind farms consisting of type 3 and type 4 wind turbines located within the distribution system has been growing rapidly. Wind turbines can be utilized as a continuous reactive power source to support the system voltage by taking advantage of their reactive power control capability. This paper aims to further develop the reactive power assignment strategy in order to minimize losses in wind farms described in the published paper. We introduce the method of reconfiguration and numbering to apply the algorithm to the wind farm structure and develop the previously-defined allocation ratio into two types of allocation ratios. The goal is to apply the loss minimization algorithm to a wind farm configuration with up to two wind turbines connected to one ring main unit (RMU). The proposed strategy reduces power loss and increases the real power flow in the wind farm by allocating reactive power to connected wind turbines taking into account the resistance value. The proposed allocation technique is validated in a Real Time Digital Simulator (RTDS)-based Hardware-in-the-loop Simulation (HILS) environment considering the Dongbok wind farm configuration in Jeju, South Korea. In the simulation, a Raspberry Pi acts as a wind farm controller sending a reactive power dispatch signal to each wind turbine via Modbus TCP/IP protocol. The simulation results mean that, applying the proposed algorithm, we can expect loss reduction effects in the wind farm.

**Keywords:** wind farm management system; reactive power control; hardware-in-the-loop simulation; RTDS; Raspberry Pi; loss minimization



**Citation:** Yoo, D.; Kang, S.; Jang, G.; Jung, S. Development of Reactive Power Allocation Method for Radial Structure Wind Farm Considering Multiple Connections. *Electronics* **2022**, *11*, 2176. <https://doi.org/10.3390/electronics11142176>

Academic Editor: Rui Castro

Received: 22 June 2022

Accepted: 9 July 2022

Published: 11 July 2022

**Publisher's Note:** MDPI stays neutral with regard to jurisdictional claims in published maps and institutional affiliations.



**Copyright:** © 2022 by the authors. Licensee MDPI, Basel, Switzerland. This article is an open access article distributed under the terms and conditions of the Creative Commons Attribution (CC BY) license (<https://creativecommons.org/licenses/by/4.0/>).

## 1. Introduction

The environmental problem and the movement toward reducing the use of fossil fuels are forcing power system planners around the globe to pursue the expansion of renewable energy. In this process, the energy distribution around the world has changed from in large part a conventional synchronous generator to a high level of inverter-based resources (IBRs). With the spread of an energy policy promoting renewable energy based on incentive legislation such as the Renewable Energy Certificate (REC), new market structures have been created with not only existing companies but also small renewable energy providers. This increase in unsupervised renewable energy may introduce uncertainty as their output characteristics depend only on the environment, causing output fluctuation [1]. Therefore, renewable energy sources are required to have the ability to control their output power, following specific regulations in order to mitigate various stability issues of the power systems.

To effectively manage renewable energy sources, a hierarchical control structure based on supervisory control and data acquisition (SCADA), has been commonly imposed on commercial power plants. This data analysis is applicable to the prediction process or active power control method in various renewable management systems, as in [2]. Particularly in large-scale wind power plants that require a wide area, SCADA is the basic configuration

for operational reliability. With the enhancement of a communication capacity in SCADA, as in [3], recent studies, such as [4,5], have developed active response plans that include the Transmission System Operator (TSO) in terms of both real/reactive power. As for real power control, improving the response to limiting signals is a primary concern for the hierarchical control structure [6]. In [7–9], the practical delay of wind farm control in the provision of ancillary services to the grid was studied and the effect of the curtailment response was simulated. The effort was seen as progress toward a stable control process as it focuses on the responsiveness of the connected power system with SCADA.

In the wind power sector, IBRs are considered to contain great potential in terms of providing reactive power. In most countries, large-scale integration of wind farms is possible with IBR, including a doubly-fed induction generator (DFIG) and a permanent magnet synchronous generator (PMSG), which can provide reactive power support. With advances in power conversion systems (PCS), various types of research have been carried out on active and reactive power support by a single wind turbine. In [10], a method of improving the transient stability condition was proposed by utilizing power injection from a wind farm, based on a modification of the rotor side converter controller. The authors in [11] proposed a coordinated active and reactive power control scheme for wind farms based on model predictive control (MPC). In [12–15], the authors proposed an operation plan in certain wind integration systems utilizing controllable devices to improve system stability.

In terms of supporting reactive power by a wind farm, grid-integrated renewable sources must comply with the designated grid code. Regarding wind energy in particular, control provisions are further subdivided, as in [16], due to concerns about output fluctuations. General wind farms connected to substations through exclusive lines are obliged to provide reactive power capability to the grid within the established curve [6,17]. In the centralized control structure, reactive power management focuses on higher class reference to handle the total extracted quantity at the common coupling point (PCC). A recently developed wind farm management system adapts the hierarchical structure to use various optimization or efficiency methods [18]. Some expanded real-time controllers using the existing communication protocols require even advanced data aggregation methods [19,20]. In addition, with the use of hierarchical control structures, practical verification of the control method and its accuracy is needed. A large-scale analysis using a Real-Time Digital Simulator (RTDS) has been established to consider real-time simulation and in the future, the impact assessment of distributed generation on the power system is likely to take the form of a corresponding structure using RTDS. Considering large-scale renewable energy, the use of RTDS is considered a remarkable emergency verification option.

TSOs have asked a power plant operator that supports reactive power to maintain an imposed objective function for a single wind farm. In this process, the proportional method which evenly divides the reference quantity among the wind turbines is widely utilized in industrial applications. However, recently created solutions consider the wide-area configuration of wind farms. As wind farms have a distribution voltage level (33 kV or less) that may cause increased cable power loss [21], various studies are trying to find a more efficient way to extract power according to the imposed reference. Along with this, previous studies have addressed the issue of mechanical torque consideration to avoid stress due to reactive power support [22], security margin in hierarchical control [23] and thermal variation of PCS [24].

Recently published work on reactive power optimization using the fast response capability of wind turbines implies that such control may contribute to the power converter lifecycle in IBRs [25]. In addition, in the optimal reactive power control scheme of [26], the consensus alternating direction method of multipliers (ADMM) is used to minimize losses of DFIG-based wind farms, and [27,28] consider an optimal reactive power dispatch strategy using artificial intelligence techniques to meet the control objective including minimization of power loss. As IBR has the ability to regulate reactive power, it is evaluated as economical to maximize the capability to provide the ancillary reactive power service.

Since IBR-based wind farms of class over 100 MW can have a large compensation reserve, as can single compensation facilities (such as STATCOM), it is likely that such capacity will be available for the operation of the electrical system. Therefore, meeting the TSO requirements encourages the additional application of reactive power management from the point of view of operational advantages for wind farm owners. A reactive power assignment strategy was introduced in [29] to minimize the loss in the radial wind farm structure, and [30] developed an optimal reactive power dispatch strategy to minimize wind farm power loss while maintaining the internal layout voltage within the operating ranges. In [29,30], the simulation took into account the radial wind farm configuration with a single wind turbine connection on one ring main unit (RMU).

This paper aims to evaluate the effect of a published management solution by performing the RTDS-based HILS (Hardware-in-the-loop simulation) verification where the RTDS model is configured based on the Dongbok wind farm configuration. By means of hierarchical control flow and the objective function in [29], we intend to confirm the adjustment availability of the published reactive power control algorithm based on the radial structure of a wind farm with multiple wind turbine connections. Furthermore, in HILS, the Raspberry Pi acts as a wind farm controller that communicates with RTDS via Modbus TCP/IP protocol to dispatch reactive power to each wind turbine. This indicates that the proposed management algorithm can find universal application in the real industry.

The paper is ordered as follows. In Section 2, we describe a framework for reactive power dispatch including the hierarchical structure of wind farm control, reactive power dispatch methodology, and the Dongbok wind farm on which simulation cases are based. In Section 3, we introduce the method of reconfiguration and numbering to apply the algorithm to the wind farm structure and develop the previously defined allocation. Section 4 presents the simulated results of this reactive power dispatch method with the various cases of different reactive power dispatch. Finally, conclusions including the tendency of the algorithm are drawn in Section 5.

## 2. Framework for Reactive Power Dispatch

### 2.1. Hierarchical Control

Hierarchical wind farm control is generally used to effectively control the reactive power of wind turbines and manage power capacity [29]. After comparing the output measured at PCC with the reference power received by the grid operator, a curtailment signal is used to control individual wind turbines, and thanks to ESS integration, it is possible to manage output control of wind turbines, hence alleviating transmission congestion [31,32]. The hierarchical wind farm management system (WFMS) measures and manages voltage fluctuations within the wind farm, including the PCC, and thus performs the reactive power control in the same hierarchical control structure. Figure 1 illustrates the hierarchical structure of reactive power control. The wind farm controller generates the set reactive power assigned to the individual turbine controller as an input signal. The wind farm controller receives information about each wind turbine and calculates the amount of power available for each of them. Once the voltage in the PCC fluctuates or a TSO transmits a signal for reactive power supply to the controller, the reactive power required for each wind turbine is allocated based on the power output at the PCC via the PI controller. In this allocation process, a simple proportional distribution method was used until recently for the convenience of calculation, but optimized allocation methods for reducing electrical loss and PCC voltage variation have been investigated in [29,30]. This paper applies an allocation technique to the radial wind farm structure with multiple wind turbine connections at each connection point in order to reduce losses that can occur in the wind farm.

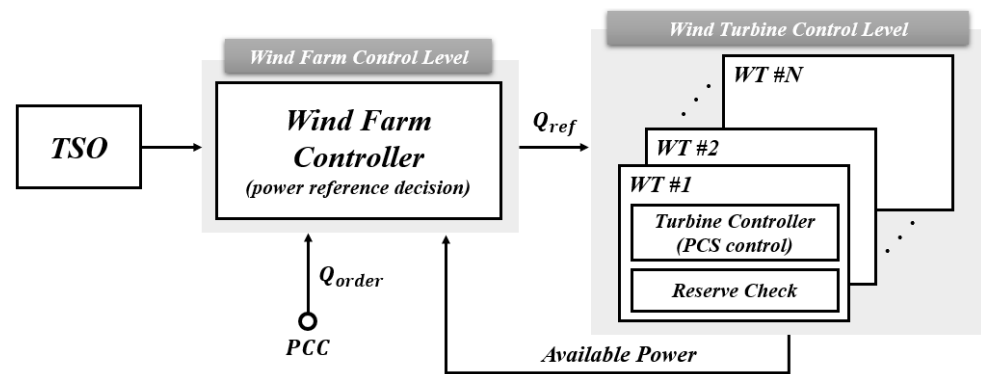


Figure 1. Centralized control structure for reactive power.

### 2.2. Reactive Power Dispatch Methodology

The WFMS hierarchical control type manages power reference management for each wind turbine. In general, the TSO can send the power dispatch signal to the WFMS in real-time considering the current condition of the system. Generally, the active power reference is determined based on the maximum power point tracking (MPPT) control, but the TSO can transfer a curtailment signal to minimize the transmission congestion or to optimize the mix of energy resources. The required amount of curtailment can be calculated, and a power dispatch signal according to the respective curtailment signal is allocated to each turbine by the WFMS. Regarding the reactive power control, it could be controlled independently, and the WFMS can expect the reactive power reserve for each wind turbine. Based on the capacity of the converter, the reactive reserve is generally calculated according to Equation (1).

$$|Q_{max}| = \sqrt{S_{pcs}^2 - P^2} \tag{1}$$

In Equation (1),  $Q_{max}$  means the reactive power reserve of the individual wind turbine, and  $S_{pcs}$  indicates its converter capacity. The reactive power reference for each turbine can be determined from the corresponding real-time calculated power reserve and the reactive power reference for the entire wind farm can be calculated according to Equation (2). In Equation (2),  $Q_{ref}$  means the reactive power output reference for each wind turbine and  $Q_{ord}$  is the reactive power reference from the TSO for the entire wind farm.

$$Q_{ord} = \sum_{l=1}^L \sum_{n=1}^{N_l} Q_{ref}(l, n) \tag{2}$$

This paper considers a loss-based reactive power allocation method to assign reactive power references to minimize the reactive power flow through the entire wind farm cable. In order to take into account the incremental transmission losses over a short period of time, reactive power is allocated proportionally to the cable parameter which has a great influence on the power loss. The power loss,  $P_{loss}$ , in the wind farm cable can be represented by Equation (3).

$$P_{loss} = I^2R = \frac{P^2 + Q^2}{V^2} \cdot r_{cab} \tag{3}$$

In Equation (3),  $r_{cab}$  means the cable resistance. A WFMS with a hierarchical control structure can allocate the reactive power considering each cable parameter that is static data. By focusing on static data rather than on time variable data, such as active power and voltage, the power loss is proportional to the square of the reactive power flow. Therefore,

Equation (4) can be configured in a wind farm where one or more wind turbines are sequentially connected to each connection point.

$$\eta = \frac{\sqrt{r_{line}}}{\sqrt{r_{con}} + \sqrt{r_{line}}} \tag{4}$$

In Equation (4),  $r_{con}$  means the resistance of the cable connected between the RMU and the wind turbine and  $r_{line}$  means the resistance of the cable between RMUs. This ratio considers the distance between the wind turbine connected to the current connection point and the next connection point. This method applies to series-connected wind turbines, but it is difficult to apply the same method to onshore wind farms where multiple wind turbines are connected to a specific node. This paper analyzes the general structure of the radial onshore wind farm and proposes a method to develop a published allocation method by reconstructing a proportional function for the general wind farm structure where there are up to two wind turbines connected on each RMU.

### 2.3. Dongbok Wind Farm

Figure 2 shows the Dongbok wind farm structure with 4 connection lines to the PCC which is connected to the bulk power system the voltage level of which is 22.9 kV. Each connection line is composed of two RMUs with one or two wind turbines connected on each RMU. The radial configuration of the wind farm, which is the main consideration of this paper, refers to the wind farm structure, to which is difficult to apply the published allocation method due to the connection of two wind turbines at a specific connection point. As multiple wind turbines at the same connection point should take charge of the reactive power required for the connection point, a reconfiguration of the published allocation method is required.

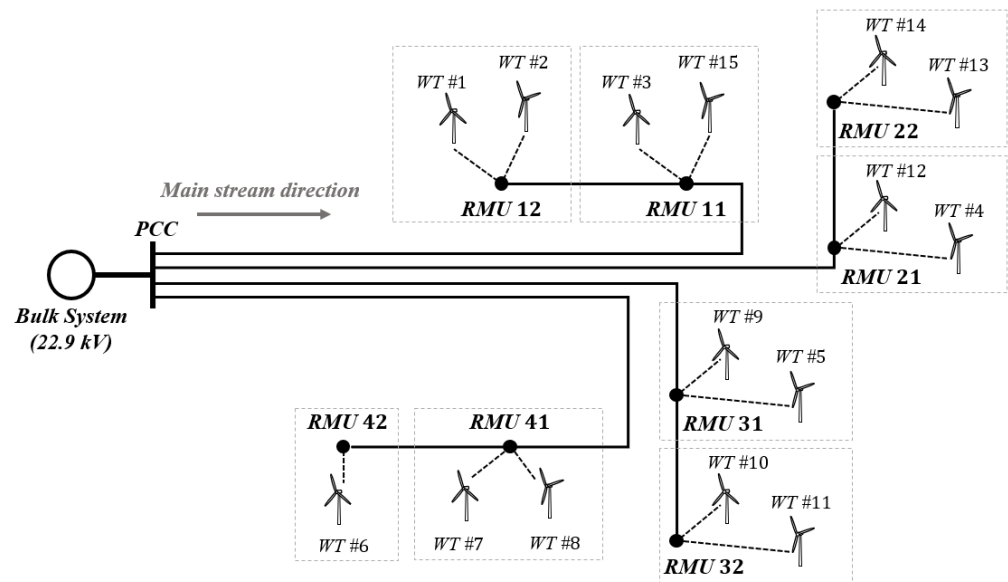


Figure 2. Exemplary structure for multiple wind turbines connection (Dongbok wind farm).

In this paper, the simulation for verification takes into account the cable parameters of the wind farm structure. Table 1 shows the RLC components of the cable. The cable information is classified by the number of RMU and the connected wind turbines. The RTDS-based simulation model is set up based on the corresponding cable information. The proposed algorithm is also based on the wind farm configuration in which up to two wind turbines are connected to one RMU model.

**Table 1.** Inner cable parameters of Dongbok wind farm.

From	To	Cable SQMM (mm <sup>2</sup> )	Length (km)	X <sub>L</sub> (Ω)	C (μF)	R (Ω)	L (mH)
1	RMU1	60	0.374	0.0651	0.0785	0.1459	0.1726
2	RMU1	60	0.08	0.0139	0.0168	0.0312	0.0369
RMU1	RMU2	100	0.061	0.0099	0.014	0.0143	0.0262
3	RMU2	60	0.357	0.0621	0.075	0.1392	0.1648
15	RMU2	60	0.27	0.0470	0.0567	0.1053	0.1246
RMU2	PCC	200	4.57	0.6718	1.4624	0.5438	1.782
14	RMU3	60	0.261	0.0454	0.0548	0.1018	0.1205
13	RMU3	60	0.21	0.0365	0.0441	0.0819	0.0969
RMU3	RMU4	100	0.297	0.0481	0.0683	0.0695	0.1276
4	RMU4	60	0.203	0.0353	0.0426	0.0792	0.0937
12	RMU4	60	0.17	0.0296	0.0357	0.0663	0.0785
RMU4	PCC	200	3.83	0.0563	1.2256	0.4558	1.4934
11	RMU5	60	0.57	0.0992	0.1197	0.2223	0.2631
10	RMU5	60	0.226	0.0393	0.0475	0.0881	0.1043
RMU5	RMU6	100	0.173	0.028	0.0398	0.0405	0.0743
5	RMU	60	0.307	0.0535	0.0645	0.1197	0.1417
9	RMU6	60	0.082	0.0143	0.0172	0.032	0.0379
RMU6	PCC	200	3.01	0.4425	0.9632	0.3582	1.1737
6	RMU7	60	0.24	0.0418	0.0504	0.0936	0.1108
RMU7	RMU8	100	0.326	0.0528	0.075	0.0763	0.1401
8	RMU8	60	0.21	0.0365	0.0441	0.0819	0.0969
7	RMU8	60	0.142	0.0247	0.0298	0.0554	0.0655
RMU8	PCC	200	2.54	0.3734	0.8128	0.3023	0.9904

### 3. Algorithm Configuration

To apply the algorithm to the Dongbok wind farm configuration, its configuration should be redefined, including the RMU and wind turbine numbering. Therefore, the reconfiguration process from the configuration in Figure 2 to the configuration in Figure 3 progresses.

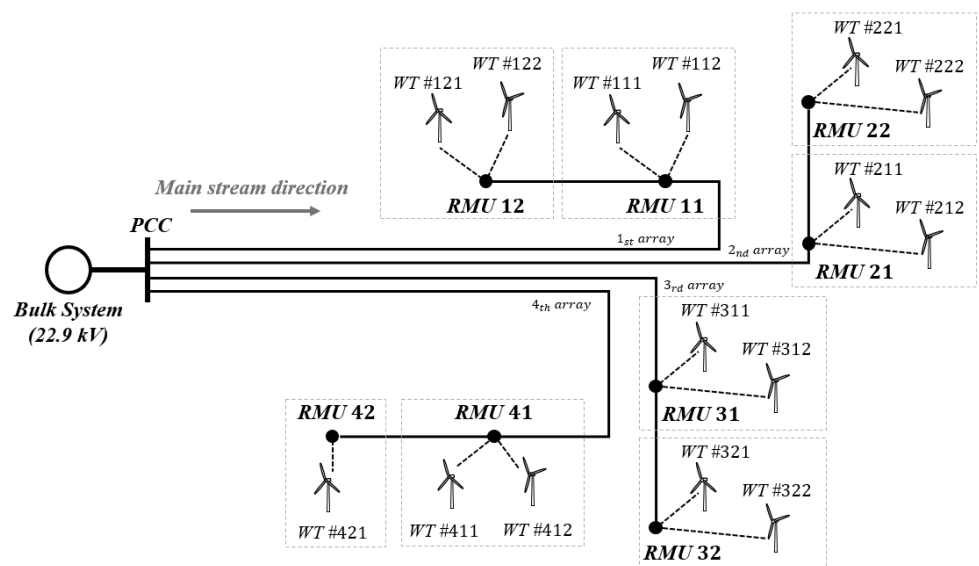


**Figure 3.** Reconfigured Dongbok wind farm structure.

The numbering method for developing equations for the Dongbok wind farm model is shown in Figure 4. For convenience, we focus on a single line connected to the PCC with multiple RMUs and wind turbines. This paper derives the reactive power allocation method by developing the reactive power reference allocation method when multiple wind

turbines are connected, and the equations for assigning the power references to multiple wind turbines connected to a specific connection point are presented below. When a single wind turbine is connected to the  $n_{th}$  RMU, the allocation ratio for the wind turbine is set based on the number of connection points as shown in Equation (5).

$$\eta_n = \frac{\sqrt{r_{n \cdot n+1}}}{\sqrt{r_{con \cdot n} + \sqrt{r_{n \cdot n+1}}}} \tag{5}$$

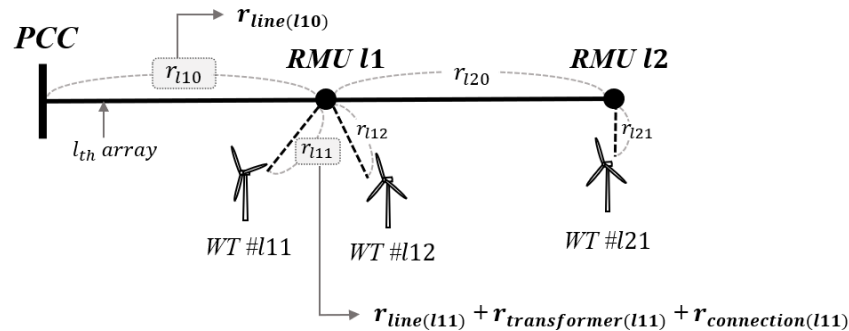


Figure 4. Wind farm numbering method to apply the algorithm.

However, for multiple wind turbine connections, the numbering system should be modified to calculate the allocation ratio as shown in Figure 4.

To execute the reactive power allocation algorithm, two types of allocation ratios are calculated as shown in Equations (6–8). After the optimization process that determines the amount of reactive power to be allocated to each array, the reactive power reference for each RMU is calculated depending on the RMU allocation ratio,  $\alpha_{lm}$ . The RMU allocation ratio is calculated as shown in Equations (6) and (7). When calculating the RMU allocation ratio on the RMU with two wind turbine connections, the parallel resistance value between the RMU and the connected wind turbines is considered to represent the resistance components connected to multiple wind turbines behind the RMUs as shown in Equation (6). When one wind turbine is connected to the RMU, the resistance between the RMU and the wind turbine ( $r_{l21}$ ) is only considered when calculating the RMU allocation ratio as shown in Equation (7). Following that, the reactive power references for the wind turbines connected to each RMU are calculated depending on the wind turbine’s allocation ratio,  $\beta_{lmn}$ . The wind turbine allocation ratios are calculated according to Equation (8). Given that in Figure 4 there is only one wind turbine connected to the second RMU, the wind turbine allocation ratio for wind turbine #121 is 1, indicating that the wind turbine is responsible for supplying the required reactive power of the RMU.

$$\alpha_{l1} = \frac{1/\sqrt{\frac{1}{r_{l11}} + \frac{1}{r_{l12}}}}{1/\sqrt{\frac{1}{r_{l11}} + \frac{1}{r_{l12}}} + 1/\sqrt{r_{l20} + r_{l21}}} \tag{6}$$

$$\alpha_{l2} = \frac{1/\sqrt{r_{l20} + r_{l21}}}{1/\sqrt{\frac{1}{r_{l11}} + \frac{1}{r_{l12}}} + 1/\sqrt{r_{l20} + r_{l21}}} \tag{7}$$

$$\beta_{l11} = \frac{1/\sqrt{r_{l11}}}{1/\sqrt{r_{l11}} + 1/\sqrt{r_{l12}}} = \frac{\sqrt{r_{l12}}}{\sqrt{r_{l11}} + \sqrt{r_{l12}}}, \beta_{l12} = \frac{\sqrt{r_{l11}}}{\sqrt{r_{l11}} + \sqrt{r_{l12}}}, \beta_{l21} = 1 \tag{8}$$

Based on the respective allocation ratios, the reactive power reference required for the  $m_{th}$  connection point from the PCC is calculated as Equation (9) and the reactive power reference required for the  $n_{th}$  wind turbine at the  $m_{th}$  connection point from the PCC is

calculated as Equation (10). In Equations (9) and (10),  $Q_{req}(l)$  denotes the reactive power required at one array and can be expressed as the sum of the reactive power required for each wind turbine as shown in Equation (8).  $Q_{ref}$  is the reactive power reference for each wind turbine, and  $Q_{loss}$  means the reactive power absorbed by the cable in the process of transferring the reactive power from the wind turbine to the connection point. Based on the configured equations, reactive power allocation can be carried out for multiple wind turbine connections at a specific point.

$$Q_{req}(l, m) = \alpha_{lm} \cdot Q_{req}(l) \tag{9}$$

$$Q_{req}(l, m, n) = \beta_{lmn} \cdot Q_{req}(l, m) = \beta_{lmn} \cdot \alpha_{lm} \cdot Q_{req}(l) \tag{10}$$

$$Q_{req \cdot l} = \sum_{i=1}^M \sum_{j=1}^{N_m} Q_{req}(l, m, n) \tag{11}$$

According to the above analysis of the allocation method, the configured algorithm is shown in Figure 5. The algorithm is configured to calculate the reactive power allocation amount in each wind turbine and mounted on the wind farm controller. The controller recognizes the current wind farm information, such as the impedance parameter and the number of connected wind turbines for each connection from PCC to the last connection point, and applies a reactive power allocation method based on the updated information. After the wind farm controller reads the real power flow and voltage information from each wind turbine, the controller optimizes the reactive power reference  $Q_{req}(l, m)$  for each RMU using Equation (12) to minimize loss across the wind farm. Then, the total amount of reactive power reference for each array is calculated by summing the reactive power required for all RMUs of the arrays. After determining a reactive power reference for each array, the reactive power reference,  $Q_{ref}$  of each wind turbine is calculated from previously calculated allocation ratios as shown in Equations (6)–(8).

$$\text{Min} \sum_{l=1}^L \sum_{m=1}^{M_i} \left[ r_{lm0} \cdot \frac{P_m(l, m)^2 + Q_{req}(l, m)^2}{V(l, m)^2} \right] \tag{12}$$



Figure 5. Flow chart of the reactive power allocation algorithm for the Dongbok wind farm.

### 4. Simulation Results

In order to apply the proposed algorithm to a commercialized wind farm, multiple turbine connections were formed in an RTDS-based simulation. The Dongbok Wind Farm, which has up to two wind turbines connected to one RMU, has four arrays with 15 wind turbines. The wind farm utilizes HJWT 2000 in [33], which is based on the DFIG type.

Figure 6 indicates the RTDS-based simulation configuration where the GTNET card of RTDS is connecting to Raspberry PI which acts as a wind farm controller via Modbus TCP/IP protocol. The wind farm controller receives a reactive power dispatch signal from TSO and based on this dispatch signal it sends a reactive power dispatch signal to each wind turbine to reduce the loss within the wind farm layout. The detailed parameters of the lines constituting the wind farm are shown in Table 1. Table 2 concerns the case study performed to confirm the application and effect of the proposed algorithm. In the proposed method, the reactive power capability of each wind turbine was calculated using Equation (1) considering the PCS capacity of each wind turbine which is 2 MVA. Therefore, each wind turbine has the same reactive power capability which is up to 1.323 MVar. In order to validate the effectiveness of the proposed method, a comparison with the case with PD method was conducted. The power loss can be measured from the simulation cases by the difference between the sum of the measured active power from each wind turbine and the measured active power flow at PCC.

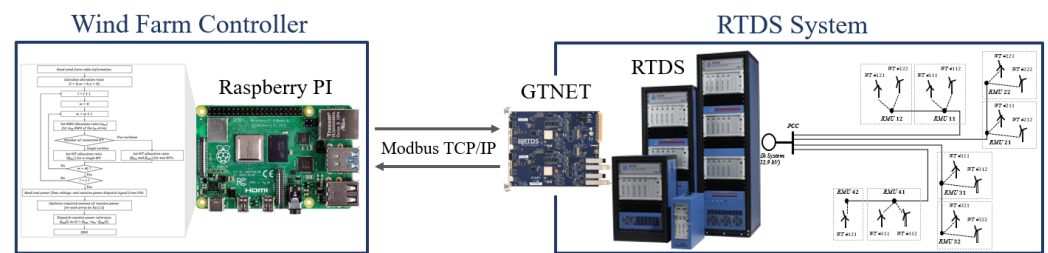


Figure 6. Simulation Configuration with RTDS and Raspberry PI.

Table 2. Case study information.

Simulated Control Methods	PD (Proportional Distribution), Proposed Method with Reactive Power Capacity Limit (See Equation (1))
Reactive power requirement	4, 6, 8, 10, 12, 14, 16 [MVar]
Active power profile	1.5 [MW] × 15 = 22.5 [MW]
Simulation time	3 [s]
Dispatch time	1 [s]

Figures 7 and 8 indicate the simulation results for the case when the step change of the reactive power reference to the wind farm occurs from the initial value (0 MVar) to the control target value (12 MVar) as shown in the relevant case study in Table 2. Figure 7 shows the real/reactive power flow and voltage at the PCC. The PCC voltage change is observed after a step change of the reactive power reference for the wind farm. After the optimization process of the reactive power allocation for each array, the reactive power references to be allocated to wind turbines are calculated by multiplying the allocation ratios as shown in Equation (9), which can be represented in Figure 8. In Figure 8d, when the assigned reactive power reference of the entire wind farm is 12 MVar, it can be seen that the calculated reactive power reference of the sixth wind turbine is beyond the reactive power capacity limit of the wind turbine, and the reactive power reference for the wind turbine is assigned a maximum output of 1.323 MVar, which is the reactive power limit in the case of 1.5 MW of real power output. It indicates that although the reactive power outputs of some wind turbines are beyond their reactive power limits; the wind farm controller reads the reactive power flow at the PCC and allocates additional reactive power to other wind turbines.

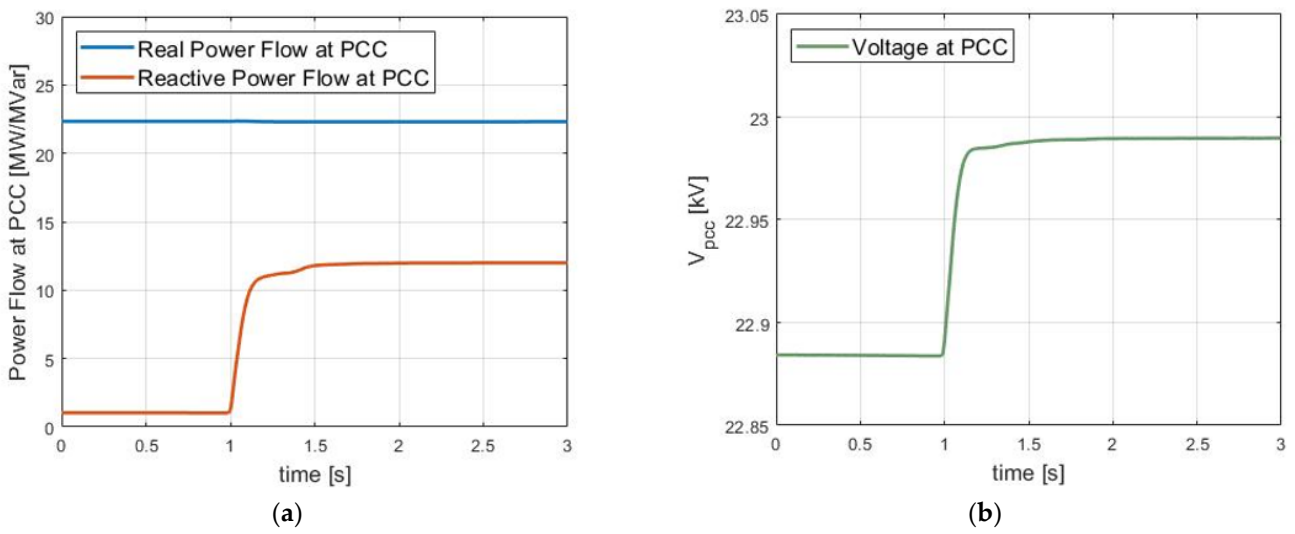


Figure 7. Simulation results: (a) Real/reactive power Flow; (b) Voltage at PCC.

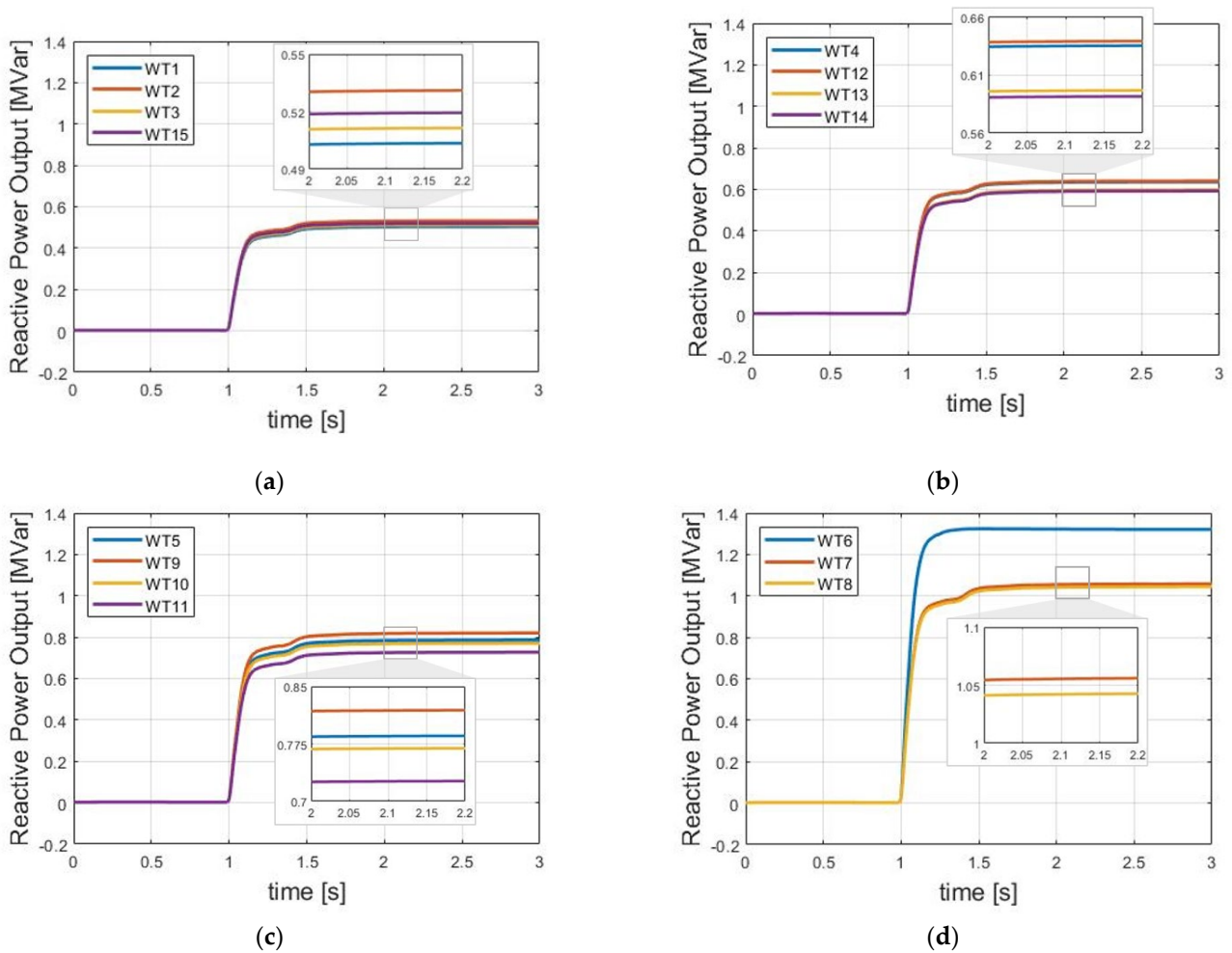


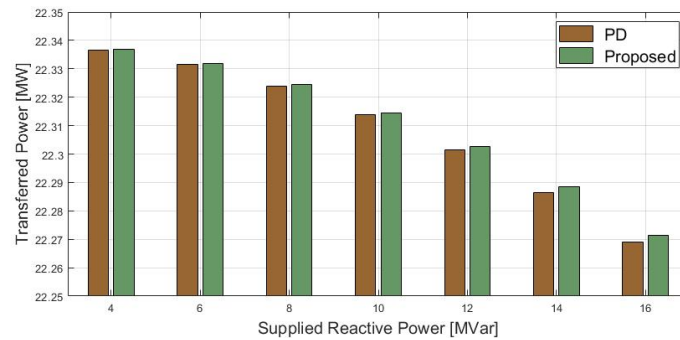
Figure 8. The reactive power outputs of wind turbines (a) array 1; (b) array 2; (c) array 3; (d) array 4.

Table 3 shows the simulation results for different reactive power requirements on the wind farm. In Table 3, the amounts of loss reduction via measured real power flow at the PCC in simulation with PD and the proposed methods, respectively, are calculated. With

the increase of the required reactive power, the loss reduction in the application of the strategy increases, as shown in Figure 9.

**Table 3.** Average real power profiles and reduced power loss.

$Q_{requirement}$ [MVar]	4	6	8	10	12	14	16
(PD) Average profile [MW]	22.33672	22.33158	22.32402	22.31396	22.30148	22.28656	22.26916
(Proposed) Average profile [MW]	22.33684	22.33183	22.32438	22.31460	22.30259	22.28850	22.27145
Loss reduction amount [kW]	0.12	0.25	0.36	0.64	1.11	1.94	2.29



**Figure 9.** Comparison of transferred active power in the case studies.

Figure 10 indicates the calculated loss occurring on each array for different reactive power requirements on the wind farm when applying PD and the proposed method. As shown in the published paper, with the increase of the reactive power requirement, the absolute value of the change in power loss increases for each array and it is observed that all the power losses for arrays are standardized.

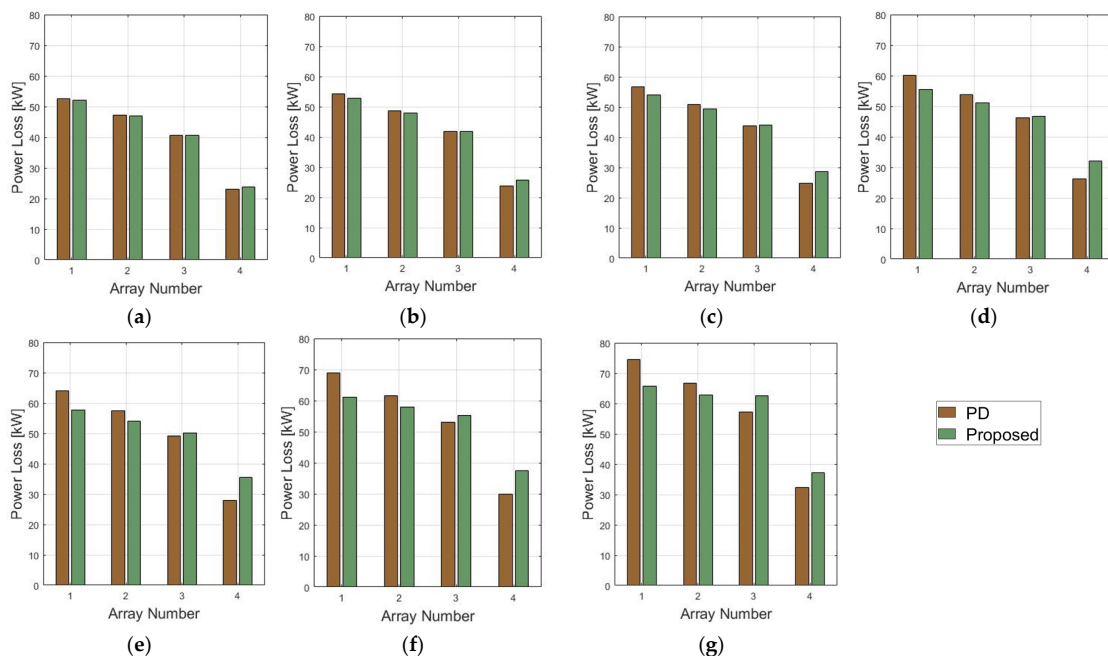


**Figure 10.** Power loss due to different reactive power dispatch signal: (a)  $Q_{pcc} = 4$  MVar; (b)  $Q_{pcc} = 6$  MVar; (c)  $Q_{pcc} = 6$  MVar; (d)  $Q_{pcc} = 8$  MVar; (e)  $Q_{pcc} = 10$  MVar; (f)  $Q_{pcc} = 12$  MVar; (g)  $Q_{pcc} = 14$  MVar.

### 5. Conclusions

This paper introduces a reactive power allocation strategy in a configured wind farm which has multiple wind turbine connections. It is done by extending and developing the

published reactive power allocation strategy to minimize wind farm losses. The RTDS model of the Dongbok wind farm was established with the specified line parameters of real layouts. The verification process was performed in a HILS environment with the designed test system and a Raspberry Pi connecting to RTDS via Modbus TCP/IP protocol. It can be concluded from the simulation results that even if many wind turbines are connected to one connection point, the proposed loss minimization algorithm contributes to the loss improvement within the wind farm when the reactive power references are allocated via the calculated reactive power allocation ratio. The study also shows the average loss comparison under the same conditions under a PD-based controller. Furthermore, the standardization of the electrical loss in the wind farm internal arrays is observed, the same effect in the application of the strategy demonstrated in the published paper. The simulation results also show a greater loss improvement for the larger amounts of reactive power that is dispatched from the TSO. This paper considers the case where a maximum of two wind turbines are connected to one connection point, but future work will take into account the applicability of the proposed algorithm in the case of further connection of wind turbines or in the case of new and different wind farm layouts.

**Author Contributions:** Conceptualization, D.Y. and S.J.; methodology, D.Y.; software, D.Y. and S.K.; validation, D.Y., S.K. and S.J.; formal analysis, D.Y. and S.J.; investigation, S.K.; writing—original draft preparation, D.Y.; writing—review and editing, S.J.; visualization, D.Y.; supervision, G.J.; project administration, S.J.; funding acquisition, S.J. All authors have read and agreed to the published version of the manuscript.

**Funding:** This work was supported by the Korea Institute of Energy Technology Evaluation and Planning Grant (No. 20207200000010) and the Korea Electric Power Corporation Grant (R21XO01-23) funded by the Korean government.

**Conflicts of Interest:** The authors declare no conflict of interest.

## Nomenclature

$Q_{max}$	Reactive power reserve of wind turbine
$S_{pcs}$	Converter capacity of wind turbine
$P$	Active power of wind turbine
$Q_{ref}$	Reactive power reference for wind turbine
$Q_{ord}$	Reactive power reference from TSO for the entire wind farm
$P_{loss}$	Power loss in wind farm
$L$	Power loss in the wind farm cable
$r_{cab}$	Cable resistance
$r_{line}$	Line resistance between RMUs
$r_{con}$	Resistance of cable connected between RMU and wind turbine
$\eta$	Allocation ratio for wind turbine
$r_{n \cdot n+1}$	Line resistance between the $n_{th}$ RMU and the $n + 1_{th}$ RMU
$r_{con \cdot n}$	Line resistance between the $n_{th}$ RMU and the connected wind turbine
$\eta_n$	Allocation ratio for wind turbine connected to the $n_{th}$ RMU
$r_{lm0}$	Reconfigured resistance consisting of $r_{line(lm0)}$
$r_{lmn}$	Reconfigured resistance consisting of $r_{line(lmn)}$ , $r_{transformer(lmn)}$ , and $r_{connection(lmn)}$
$r_{line(lm0)}$	line resistance between the $m - 1_{th}$ RMU and the $m_{th}$ RMU in the $l_{th}$ array
$r_{line(lmn)}$	line resistance between the $m_{th}$ RMU and the $n_{th}$ wind turbine connected to the $m_{th}$ RMU in the $l_{th}$ array

$r_{transformer(lmn)}$	line resistance between the $m_{th}$ RMU and the $n_{th}$ wind turbine connected to the $m_{th}$ RMU in the $l_{th}$ array
$r_{connection(lmn)}$	line resistance by connection height of the $n_{th}$ wind turbine connected to the $m_{th}$ RMU in the $l_{th}$ array
$\alpha_{lm}$	RMU allocation ratio for the $m_{th}$ RMU in the $l_{th}$ array
$\beta_{lmn}$	Wind turbine allocation ratio for the for the $n_{th}$ wind turbine connected to the $m_{th}$ RMU in the $l_{th}$ array
$Q_{req}(l)$	Reactive power required at the $l_{th}$ array
$Q_{req}(l, m)$	Reactive power required at the $m_{th}$ RMU in the $l_{th}$ array
$Q_{req}(l, m, n)$	Reactive power required for the $n_{th}$ wind turbine connected to the $m_{th}$ RMU in the $l_{th}$ array
$Q_{loss}(l, m, n)$	Reactive power loss between the $m_{th}$ RMU and the $n_{th}$ wind turbine connected to the $m_{th}$ RMU
$Q_{ref}(l, m, n)$	Reactive power required for the $n_{th}$ wind turbine connected to the $m_{th}$ RMU in the $l_{th}$ array considering reactive power loss
$P_m(l, m)$	Measured value of active power flow at the $m_{th}$ RMU in the $l_{th}$ array

## References

- Kusiak, A.; Zheng, H.; Song, Z. Short-Term Prediction of Wind Farm Power: A Data Mining Approach. *IEEE Trans. Energy Convers.* **2009**, *24*, 125–136. [CrossRef]
- Sideratos, G.; Hatziargyriou, N.D. An Advanced Statistical Method for Wind Power Forecasting. *IEEE Trans. Power Syst.* **2007**, *22*, 258–265. [CrossRef]
- Tautz-Weinert, J.; Watson, S. Using SCADA data for wind turbine condition monitoring—A review. *IET Renew. Power Gener.* **2016**, *11*, 382–394. [CrossRef]
- Huang, S.; Wu, Q.; Bao, W.; Hatziargyriou, N.D.; Ding, L.; Rong, F. Hierarchical Optimal Control for Synthetic Inertial Response of Wind Farm Based on Alternating Direction Method of Multipliers. *IEEE Trans. Sustain. Energy* **2020**, *12*, 25–35. [CrossRef]
- Cui, H.; Li, X.; Wu, G.; Song, Y.; Liu, X.; Luo, D. MPC Based Coordinated Active and Reactive Power Control Strategy of DFIG Wind Farm with Distributed ESSs. *Energies* **2021**, *14*, 3906. [CrossRef]
- The Grid Code (Issue 5, Revision 18). Available online: <https://www.nationalgrid.com/> (accessed on 20 June 2022).
- Revel, G.; Leon, A.E.; Alonso, D.M.; Moiola, J.L. Dynamics and Stability Analysis of a Power System With a PMSG-Based Wind Farm Performing Ancillary Services. *IEEE Trans. Circuits Syst. I Regul. Pap.* **2014**, *61*, 2182–2193. [CrossRef]
- Shi, X.; Cao, Y.; Shahidehpour, M.; Li, Y.; Wu, X.; Li, Z. Data-Driven Wide-Area Model-Free Adaptive Damping Control with Communication Delays for Wind Farm. *IEEE Trans. Smart Grid* **2020**, *11*, 5062–5071. [CrossRef]
- Nan, J.; Yao, W.; Wen, J.; Peng, Y.; Fang, J.; Ai, X.; Wen, J. Wide-area power oscillation damper for DFIG-based wind farm with communication delay and packet dropout compensation. *Int. J. Electr. Power Energy Syst.* **2020**, *124*, 106306. [CrossRef]
- Mitra, A.; Chatterjee, D. Active Power Control of DFIG-Based Wind Farm for Improvement of Transient Stability of Power Systems. *IEEE Trans. Power Syst.* **2015**, *31*, 82–93. [CrossRef]
- Guo, Y.; Gao, H.; Wu, Q.; Østergaard, J.; Yu, D.; Shahidehpour, M. Distributed coordinated active and reactive power control of wind farms based on model predictive control. *Int. J. Electr. Power Energy Syst.* **2019**, *104*, 78–88. [CrossRef]
- Yoon, D.H.; Song, H.; Jang, G.; Joo, S.K. Smart operation of HVDC systems for large penetration of wind energy re-sources. *IEEE Trans. Smart Grid.* **2013**, *4*, 359–366. [CrossRef]
- Huang, S.; Wu, Q.; Liao, W.; Wu, G.; Li, X.; Wei, J. Adaptive Droop-Based Hierarchical Optimal Voltage Control Scheme for VSC-HVdc Connected Offshore Wind Farm. *IEEE Trans. Ind. Inform.* **2021**, *17*, 8165–8176. [CrossRef]
- Mehrabankhomartash, M.; Saeedifard, M.; Yazdani, A. Adjustable Wind Farm Frequency Support Through Multi-Terminal HVDC Grids. *IEEE Trans. Sustain. Energy* **2021**, *12*, 1461–1472. [CrossRef]
- Wu, X.; Wang, M.; Shahidehpour, M.; Feng, S.; Chen, X. Model-Free Adaptive Control of STATCOM for SSO Mitigation in DFIG-Based Wind Farm. *IEEE Trans. Power Syst.* **2021**, *36*, 5282–5293. [CrossRef]
- Photovoltaics, D.G.; Storage, E. IEEE standard for interconnection and interoperability of distributed energy resources with associated electric power systems interfaces. *IEEE Std* **2018**, *1547*, 1547–2018.
- Desk Study on Technical Gaps of Country-Specific Grid Codes and Regulations and Recommendation for a Common Asean Wide-Grid Code, USAID. 2021. Available online: [https://pdf.usaid.gov/pdf\\_docs/PA00XVJB.pdf](https://pdf.usaid.gov/pdf_docs/PA00XVJB.pdf) (accessed on 20 June 2022).
- Wang, N.; Li, J.; Hu, W.; Zhang, B.; Huang, Q.; Chen, Z. Optimal reactive power dispatch of a full-scale converter based wind farm considering loss minimization. *Renew. Energy* **2019**, *139*, 292–301. [CrossRef]
- Sharaf, H.M.; Zeineldin, H.H.; El-Saadany, E. Protection Coordination for Microgrids with Grid-Connected and Islanded Capabilities Using Communication Assisted Dual Setting Directional Overcurrent Relays. *IEEE Trans. Smart Grid* **2016**, *9*, 143–151. [CrossRef]
- Zamani, M.A.; Yazdani, A.; Sidhu, T.S. A Communication-Assisted Protection Strategy for Inverter-Based Medium-Voltage Microgrids. *IEEE Trans. Smart Grid* **2012**, *3*, 2088–2099. [CrossRef]

21. Zhang, B.; Hu, W.; Hou, P.; Tan, J.; Soltani, M.; Chen, Z. Review of Reactive Power Dispatch Strategies for Loss Minimization in a DFIG-based Wind Farm. *Energies* **2017**, *10*, 856. [[CrossRef](#)]
22. Zhang, B.; Hou, P.; Hu, W.; Soltani, M.; Chen, C.; Chen, Z. A Reactive Power Dispatch Strategy With Loss Minimization for a DFIG-Based Wind Farm. *IEEE Trans. Sustain. Energy* **2016**, *7*, 914–923. [[CrossRef](#)]
23. Lu, Y.; Tomsovic, K. Wide area hierarchical voltage control to improve security margin for systems with high wind penetration. *IEEE Trans. Power Syst.* **2018**, *33*, 6218–6228. [[CrossRef](#)]
24. Zhou, D.; Blaabjerg, F.; Lau, M.; Tonnes, M. Thermal Behavior Optimization in Multi-MW Wind Power Converter by Reactive Power Circulation. *IEEE Trans. Ind. Appl.* **2013**, *50*, 433–440. [[CrossRef](#)]
25. Tan, H.; Li, H.; Yao, R.; Zhou, Z.; Liu, R.; Wang, X.; Zheng, J. Reactive-voltage coordinated control of offshore wind farm considering multiple optimization objectives. *Int. J. Electr. Power Energy Syst.* **2021**, *136*, 107602. [[CrossRef](#)]
26. Huang, S.; Li, P.; Wu, Q.; Li, F.; Rong, F. ADMM-based distributed optimal reactive power control for loss minimization of DFIG-based wind farms. *Int. J. Electr. Power Energy Syst.* **2020**, *118*, 105827. [[CrossRef](#)]
27. Liu, Y.; Četenović, D.; Li, H.; Gryazina, E.; Terzija, V. An optimized multi-objective reactive power dispatch strategy based on improved genetic algorithm for wind power integrated systems. *Int. J. Electr. Power Energy Syst.* **2021**, *136*, 107764. [[CrossRef](#)]
28. Xiao, Y.; Wang, Y.; Sun, Y. Reactive Power Optimal Control of a Wind Farm for Minimizing Collector System Losses. *Energies* **2018**, *11*, 3177. [[CrossRef](#)]
29. Jung, S.; Jang, G. A Loss Minimization Method on a Reactive Power Supply Process for Wind Farm. *IEEE Trans. Power Syst.* **2016**, *32*, 3060–3068. [[CrossRef](#)]
30. Yoo, Y.; Jung, S.; Song, S.; Suh, J.; Lee, J.; Jang, G. Development of practical allocation method for reactive power reference for wind farms through inner-voltage restriction. *IET Gener. Transm. Distrib.* **2022**, *16*, 3069–3079. [[CrossRef](#)]
31. Vargas, L.S.; Bustos-Turu, G.; Larrain, F. Wind Power Curtailment and Energy Storage in Transmission Congestion Management Considering Power Plants Ramp Rates. *IEEE Trans. Power Syst.* **2014**, *30*, 2498–2506. [[CrossRef](#)]
32. Prajapati, V.K.; Mahajan, V.; Padhy, N.P. Congestion management of integrated transmission and distribution network with RES and ESS under stressed condition. *Int. Trans. Electr. Energy Syst.* **2021**, *31*, e12757. [[CrossRef](#)]
33. Wind-Turbine-Models.com, Hanjin HJWT2000/87. Available online: <https://en.wind-turbine-models.com/turbines/1157-hanjin-hjwt2000-87#datasheet> (accessed on 20 June 2022).